Available online at www.sciencedirect.com
SCIENCE DIRECT®
Journal of Sound and Vibration 283 (2005) 927–941
JOURNAL OF SOUND AND VIBRATION
www.elsevier.com/locate/jsvi

On the selection of acoustic/vibration sensors for leak detection in plastic water pipes

Y. Gao[a,*], M.J. Brennan[a], P.F. Joseph[a], J.M. Muggleton[a], O. Hunaidi[b]

[a]*Institute of Sound and Vibration Research, University of Southampton, Southampton SO17 1BJ, UK*
[b]*National Research Council of Canada, Institute for Research in Construction, Ottawa, Canada K1A 0R6*

Received 4 September 2003; received in revised form 21 April 2004; accepted 20 May 2004
Available online 17 September 2004

Abstract

Leaks from buried water distribution pipes are commonly located by applying the correlation technique to two measured acoustic/vibration signals on either side of a leak. The effectiveness of the correlation technique for locating leaks in plastic pipes depends on the type of sensors used and their sensitivities. Based on an analytical model of the cross-correlation of pressure responses established in an earlier study, this paper investigates the behaviour of the cross-correlation coefficient for leak signals measured using pressure, velocity and acceleration sensors. Theoretical predictions show that a measure of pressure responses using hydrophones is effective for measurements where there is a small signal-to-noise ratio (SNR), but a sharper peak correlation coefficient can be achieved if accelerometers are used. The theoretical work is validated to some extent with test data from actual water pipes on a test site in Canada.

1. Introduction

Leaks from water supply pipes generate noise, which can be used for leak detection and location. To achieve this the correlation technique is commonly used [1–3]. However, in general, satisfactory results have only been achieved with metal pipes. Plastic pipes have proved to be

*Corresponding author. Tel: +44-023-8059-3756; fax: +44-023-8059-3190.
E-mail address: gy@isvr.soton.ac.uk (Y. Gao).

0022-460X/$ - see front matter
doi:10.1016/j.jsv.2004.05.004

problematic, since the acoustic signals in these pipes are heavily attenuated and generally narrow-band and of low frequency.

Recent work by Hunaidi and Chu [4,5] on typical plastic water distribution pipes has focused on the dominant low-frequency signals. They carried out an experimental investigation into the acoustic characteristics of several types of realistic leaks simulated under controlled conditions and found that most leak noise is concentrated at low frequencies. Moreover, they found that the effectiveness of the correlation technique is affected by the selection of acoustic/vibration sensors and the cut-off frequencies of high- and low-pass digital filters used to remove noise.

Based on a theoretical formulation of wave propagation in a fluid-filled pipe in vacuo given in Ref. [6], and the assumption that the leak source spectrum is flat in the bandwidth of interest, an analytical model of the cross-correlation function of pressure responses was developed by the authors in Ref. [7]. The model was used to show the importance of the cut-off frequency of the high-pass filter and the relative insensitivity of the correlation to the cut-off frequency of the low-pass filter for hydrophone-measured leak signals. The model also provided an understanding of the effect of the ratio of sensor distances from the leak on the correlation level.

The effectiveness of the correlation technique for locating leaks depends on the type of leak sensors used and their sensitivities [8]. It has been found that hydrophones can locate leaks with lower acoustic signals than can be located with accelerometers. In general, the greater the sensitivity of the sensor and the lower its noise floor, the smaller the leaks that can be located. Using the analytical model derived in Ref. [7], this paper investigates the use of pressure, velocity and acceleration sensors on the correlation of leak noise in plastic pipes, and compares theoretical predictions with some test data from actual water pipes. A model of wave propagation in fluid-filled plastic pipes is briefly discussed in Appendix A. Since the effectiveness of the correlation technique is greatly influenced by background noise, the effect of the background noise on the model is discussed in Appendix B.

2. Leak detection using correlation

The cross-correlation technique for source location is relatively straightforward. Vibration or acoustic signals are measured using either accelerometers or hydrophones at two access points, on either side of the location of a suspected leak. The signals from the sensors are input to the leak noise correlator, which computes the cross-correlation function of the two signals and presents the results to an operator. Fig. 1 depicts a typical measurement arrangement for a leak in a buried water pipe. An access point (normally a fire hydrant) where a sensor can be attached is located on each side of the leak at distances d_1 and d_2. In the analysis presented in this paper the pipe is assumed to be of infinite length without reflecting discontinuities for the predominantly fluid-borne wave [6], at all frequencies of interest.

Consider the situation where the data measured are two continuous random signals $x_1(t)$ and $x_2(t)$, which are assumed to be stationary (ergodic). Setting the mean value of each signal to zero, the cross-correlation function is defined by [9]

$$R_{x_1x_2}(\tau) = E[x_1(t)x_2(t+\tau)], \tag{1}$$

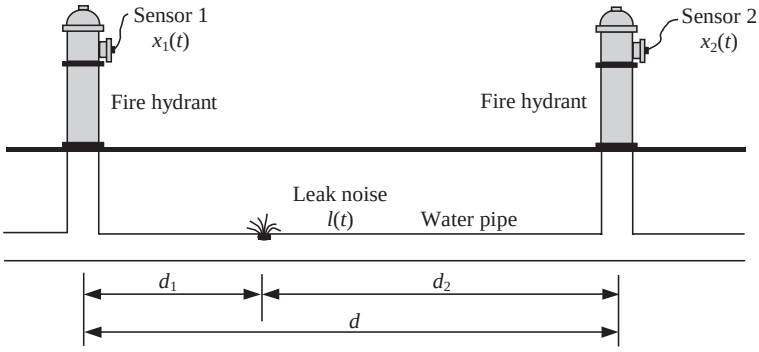

Fig. 1. Schematic of a pipe with a leak bracketed by two sensors.

where τ is the lag of time; and $E[\,]$ is the expectation operator. The argument τ that maximises Eq. (1) provides an estimate of the time delay τ_{peak}. It is useful to express the cross-correlation function in normalised form, which has a scale of -1 to $+1$, namely the correlation coefficient $\rho_{x_1x_2}(\tau)$ defined as

$$\rho_{x_1x_2}(\tau) = \frac{R_{x_1x_2}(\tau)}{\sqrt{R_{x_1x_1}(0)R_{x_2x_2}(0)}}, \tag{2}$$

where $R_{x_1x_1}(0)$ and $R_{x_2x_2}(0)$ are the values of auto-correlation functions at $\tau = 0$.

If a leak exists between the two sensor positions, a distinct peak may be found in the cross-correlation function. This gives the time delay τ_{peak} that corresponds to the difference in arrival times between the signals at each sensor. The location of the leak relative to one of the measurement points is easily calculated using the simple algebraic relationship between the time delay τ_{peak}, the distance d between the access points, and the propagation wavespeed c in the buried pipe,

$$d_1 = \frac{d - c\tau_{\text{peak}}}{2}. \tag{3}$$

3. Cross-correlation using pressure, velocity and acceleration responses

Leak noise in water-filled plastic pipes is concentrated at low frequencies, generally less than 200 Hz. In this frequency range the predominantly fluid-borne axisymmetric wave carries most of the acoustic energy generated by the leak [6,10]. The characteristics of this wave are discussed in Appendix A. In this section, models of the cross-correlation functions for pressure, velocity and acceleration responses are derived and discussed.

The frequency response function between the pressure measured at the sensor location and at the leak location, $H^p(\omega, x)$, is given by [7]

$$H^p(\omega, x) = \mathrm{e}^{-\mathrm{i}\omega x/c}\mathrm{e}^{-\omega\beta x}, \tag{4}$$

where x is the distance between the leak and sensor signals, and β is a measure of the loss within the pipe wall, as discussed in Appendix A. At low frequencies, well below the pipe ring frequency, the internal pressure amplitude, P, is related to the radial wall displacement amplitude, W, by [6]

$$W = \frac{Pa^2}{Eh}, \tag{5}$$

where E is the Young's modulus of the pipe wall, a and h are the mean pipe radius and pipe wall thickness respectively. Eq. (5) shows that there is a linear relationship between the pipe wall displacement and the internal pressure. The frequency response function between the velocity measured at the sensor location and the pressure at the leak location, $H^v(\omega, x)$, is given by

$$H^v(\omega, x) = \mathrm{i}\frac{a^2\omega}{Eh} H^p(\omega, x), \tag{6}$$

and the frequency response function of the acceleration measured at the sensor location and the pressure at the leak location, $H^a(\omega, x)$, is given by

$$H^a(\omega, x) = -\frac{a^2\omega^2}{Eh} H^p(\omega, x). \tag{7}$$

The frequency response functions given by Eqs. (4), (6) and (7) can be written in general form as

$$H(\omega, x) = (\mathrm{i}\omega)^n A_n \mathrm{e}^{-\mathrm{i}\omega x/c}\mathrm{e}^{-\omega\beta x}. \tag{8}$$

When $n = 0$, 1 and 2, Eq. (8) gives the frequency response functions of pressure, velocity and acceleration, respectively. Here $A_0 = 1$ and $A_1 = A_2 = a^2/(Eh)$. Fig. 2 shows the frequency response functions given by Eq. (8), where all the frequency response functions are normalised to their respective maximum amplitudes. The frequency response function of pressure, $H^p(\omega, x)$, given by Eq. (4) decreases exponentially with increasing frequency, so acts as a low-pass filter whereby higher frequencies are attenuated at a faster rate than low frequencies. In contrast, both the frequency response functions of velocity, $H^v(\omega, x)$, and acceleration, $H^a(\omega, x)$, given by Eqs. (6) and (7), respectively, behave as band-pass filters, with the latter having a higher "centre" frequency and a broader bandwidth, thus allowing more high frequency information to pass.

Referring to Fig. 1, the cross-spectral density $S_{x_1x_2}(\omega)$ for two signals $x_1(t)$ and $x_2(t)$ measured at positions $x = d_1$ and $x = d_2$, is given by

$$\begin{aligned} S_{x_1x_2}(\omega) &= \frac{1}{2\pi}\lim_{T\to\infty} E\left[\frac{X^*_{1T}(\omega)X_{2T}(\omega)}{T}\right] \\ &= S_{ll}(\omega)H^*(\omega, d_1)H(\omega, d_2), \end{aligned} \tag{9}$$

where $S_{ll}(\omega)$ is the auto-spectral density of the leak pressure signal $l(t)$. Combining Eq. (8) with Eq. (9) gives the cross-spectral density as

$$S_{x_1x_2}(\omega) = A_n^2 S_{ll}(\omega)\Psi_{2n}(\omega)\mathrm{e}^{\mathrm{i}\omega T_0}, \tag{10}$$

where $\Psi_{2n}(\omega) = \omega^{2n}\Psi(\omega)$; $\Psi(\omega) = |H^{p*}(\omega, d_1)H^p(\omega, d_2)| = \mathrm{e}^{-\omega\beta d}$; $T_0 = -(d_2 - d_1)/c$ is the time delay; and $d = d_1 + d_2$. When $n = 0$, 1 and 2, Eq. (10) gives the cross-spectral density for pressure, velocity and acceleration signals respectively. The corresponding phase spectrum that is related to

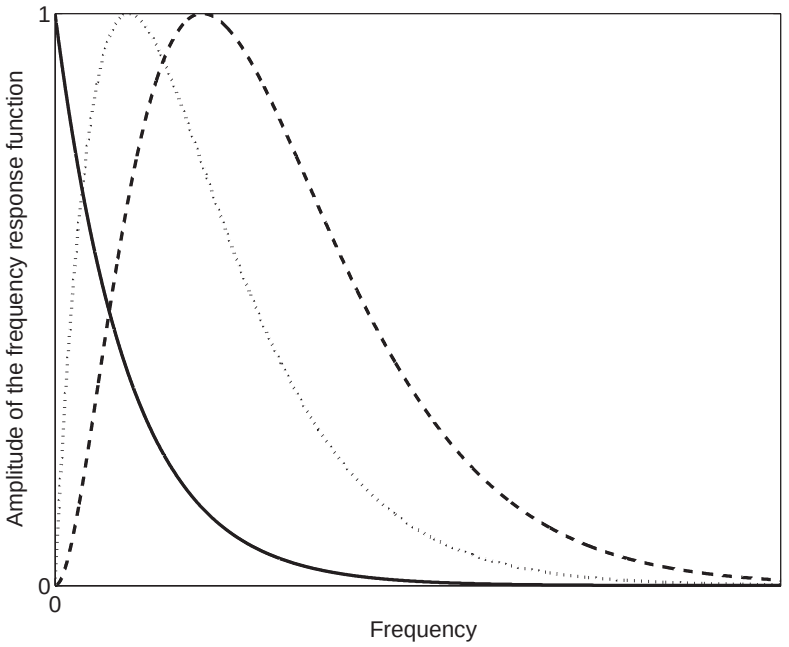

Fig. 2. Illustration of the amplitude of the transfer function. All the frequency responses are normalised to the corresponding maximum amplitudes. Pressure (—), velocity (……) and acceleration (----).

the time shift experienced by the signals as they propagate along the pipe, is given by

$$\Phi_{x_1x_2}(\omega) = \arg\{S_{x_1x_2}(\omega)\} = \omega T_0. \tag{11}$$

It is clear from Eq. (11) that the phase spectrum is independent of the choice of acoustic/vibration sensors.

Since multiplication in one domain is a convolution in the transformed domain, the cross-correlation function between the measured signals $R_{x_1x_2}(\tau)$ is given by

$$\begin{aligned} R_{x_1x_2}(\tau) &= F^{-1}\{S_{x_1x_2}(\omega)\} \\ &= A_n^2 R_{ll}(\tau) \otimes \psi_{2n}(\tau) \otimes \delta(\tau + T_0), \end{aligned} \tag{12}$$

where $F^{-1}\{\}$ denotes the inverse Fourier transform, $\otimes$ denotes convolution, $R_{ll}(\tau) = F^{-1}\{S_{ll}(\omega)\}$ is the auto-correlation of the leak signal, $\psi_{2n}(\tau) = F^{-1}\{\Psi_{2n}(\omega)\}$, and $\delta(\tau)$ is the Dirac delta function. An interpretation of Eq. (12) is that the delta function $\delta(\tau + T_0)$ is broadened by the introduction of the leak spectrum $S_{ll}(\omega)$ and the frequency behaviour of $\Psi_{2n}(\omega)$. Thus, even if $S_{ll}(\omega)$ is a constant S_0, the delta function is smeared because of the frequency attenuation of the leak signal. Reliable leak detection can only be accomplished when a peak can be distinguished in the cross-correlation function. A sharp peak rather than a smeared broad one is required to achieve accurate estimation of the time delay. Because the behaviour of $\Psi_{2n}(\omega)$ is governed by the choice of acoustic/vibration sensors, selection of appropriate sensors may offer improvement of the time delay estimation from the cross-correlation of the leak noise. This is addressed below.

The relationship $\psi_{2n}(\tau) = F^{-1}\{\Psi_{2n}(\omega)\}$ may be rewritten as

$$\psi_{2n}(\tau) = (-1)^n \frac{\mathrm{d}^{2n}\psi(\tau)}{\mathrm{d}\tau^{2n}}, \tag{13}$$

where

$$\psi(\tau) = F^{-1}\{\Psi(\omega)\} = \frac{\beta d}{\pi[(\beta d)^2 + \tau^2]}.$$

Eq. (12) can thus be reformulated as

$$R_{x_1x_2}(\tau) = (-1)^n A_n^2 R_{ll}(\tau) \otimes \frac{\mathrm{d}^{2n}\psi(\tau)}{\mathrm{d}\tau^{2n}} \otimes \delta(\tau + T_0). \tag{14}$$

If it is assumed that $S_{ll}(\omega) = S_0$, Eq. (14) becomes

$$R_{x_1x_2}(\tau) = (-1)^n A_n^2 S_0 \frac{\mathrm{d}^{2n}\psi(\tau + T_0)}{\mathrm{d}\tau^{2n}}. \tag{15}$$

Following a similar analysis to that for the cross-correlation function of two sensor signals, the auto-correlation function is given by

$$R_{xx}(\tau) = (-1)^n A_n^2 S_0 \frac{\mathrm{d}^{2n}\varphi(\tau)}{\mathrm{d}\tau^{2n}}, \tag{16}$$

where

$$\varphi(\tau) = F^{-1}\{\Gamma(\omega)\} = \frac{2\beta x}{\pi[(2\beta x)^2 + \tau^2]}.$$

Combining Eqs. (15), (16) with (2) gives the cross-correlation coefficient as

$$\rho_{x_1x_2}(\tau) = \frac{\dfrac{\mathrm{d}^{2n}\psi(\tau + T_0)}{\mathrm{d}\tau^{2n}}}{\sqrt{\left.\dfrac{\mathrm{d}^{2n}\varphi(0)}{\mathrm{d}\tau^{2n}}\right|_{x=d_1} \left.\dfrac{\mathrm{d}^{2n}\varphi(0)}{\mathrm{d}\tau^{2n}}\right|_{x=d_2}}}. \tag{17}$$

The corresponding correlation coefficients for pressure, velocity and acceleration signals, are discussed below:

1. For pressure signals, setting $n = 0$, Eq. (17) becomes

$$\rho_{x_1x_2}(\tau) = \frac{2\sqrt{d_1 d_2}}{d} \frac{(\beta d)^2}{(\beta d)^2 + (\tau + T_0)^2}. \tag{18a}$$

2. Setting $n = 1$ for velocity signals, Eq. (17) becomes

$$\rho_{x_1x_2}(\tau) = \left(\frac{2\sqrt{d_1d_2}}{d}\right)^3 \left[\frac{(\beta d)^2}{(\beta d)^2 + (\tau + T_0)^2}\right]^2 \times \left\{1 - \frac{4(\tau + T_0)^2}{(\beta d)^2 + (\tau + T_0)^2}\right\}^2. \tag{18b}$$

3. Setting $n = 2$ for acceleration signals, Eq. (17) becomes

$$\rho_{x_1x_2}(\tau) = \left(\frac{2\sqrt{d_1d_2}}{d}\right)^5 \left[\frac{(\beta d)^2}{(\beta d)^2 + (\tau + T_0)^2}\right]^3 \times \left\{1 - \frac{12(\tau + T_0)^2}{(\beta d)^2 + (\tau + T_0)^2} + \frac{16(\tau + T_0)^4}{\left[(\beta d)^2 + (\tau + T_0)^2\right]^2}\right\}. \tag{18c}$$

Consider the following two cases:

(i) When $d_1 \neq d_2 \neq 0$, the peak cross-correlation coefficients for pressure, velocity and acceleration responses are all less than 1, with the greatest value being for pressure signals and the smallest for acceleration signals. The sharpest peak, however, is exhibited by the cross-correlation of the acceleration signals and the broadest one exhibited by the correlation of the pressure signals. This can be seen in Fig. 3(a) for the case of $d_1/d_2 = 2.5$.

(ii) When $d_1 = d_2 \neq 0$, the peak cross-correlation coefficients for pressure, velocity and acceleration responses are all equal to unity, as can be seen from Fig. 3(b). This means that the two responses are identical in each case.

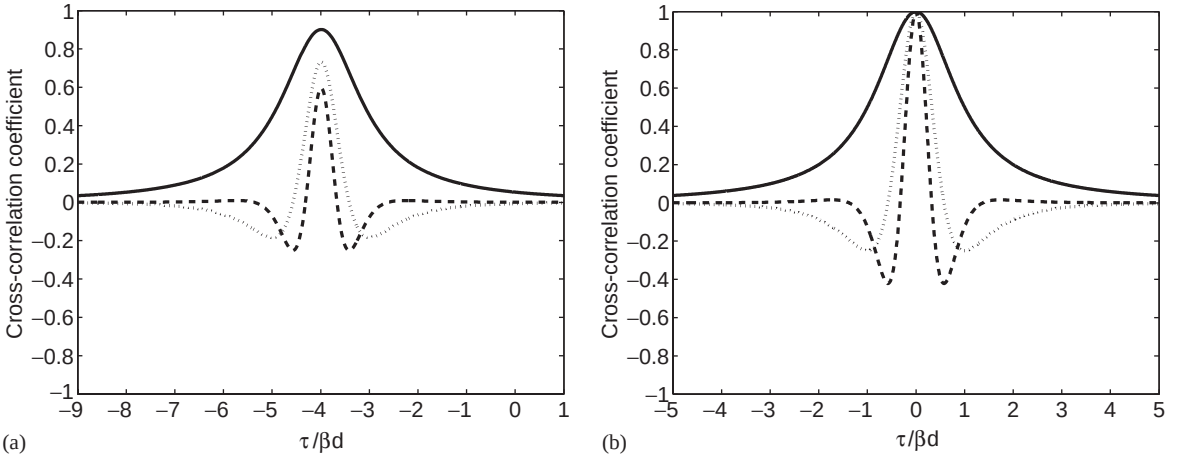

Fig. 3. Cross-correlation coefficients using pressure (—), velocity (……) and acceleration (----): (a) $d_1/d_2 = 2.5$; (b) $d_1 = d_2$.

To clarify further the effect of the selection of acoustic/vibration sensors on the correlation technique, the peak cross-correlation coefficient is investigated. When $\tau = -T_0$, Eqs. (18a–c) reduce to,

$$\rho_{x_1x_2}(\tau_{\text{peak}}) = \left(\frac{2\sqrt{d_1 d_2}}{d}\right)^{2n+1} = \left(\frac{2\sqrt{d_1/d_2}}{1 + d_1/d_2}\right)^{2n+1}. \tag{19}$$

Eqs (18a–c) show that the correlation coefficients are dominated by both the loss of the pipe, β, and the locations of two sensors, d_1 and d_2. Interestingly, the peak values of the correlation coefficients given by Eq. (19) are only related to the ratio of the relative distances d_1/d_2, and not on their absolute values. Fig. 4 shows the peak values of the cross-correlation coefficients given by Eq. (19) as a function of d_1/d_2. As discussed previously it can be seen that for two equispaced sensors, the peak cross-correlation coefficients are all unity. Altering the ratio d_1/d_2, the peak value of the pressure responses changes slowly by comparison with those given by the velocity and acceleration responses. This shows that for leak detection measurements, where $d_1 \neq d_2$, which is the most likely situation in practice, the pressure signals give the largest cross-correlation coefficient. Moreover, good levels of correlation (e.g., greater than about 0.5) are only possible when the ratio of distances satisfy $1/10 \leqslant d_1/d_2 \leqslant 10$, $1/4 \leqslant d_1/d_2 \leqslant 4$ and $1/3 \leqslant d_1/d_2 \leqslant 3$ for pressure, velocity and acceleration responses, respectively. Otherwise, the peak correlation values of the velocity and acceleration responses rapidly become very small. Therefore, for low levels of leak signals, namely in a small signal to noise ratio (SNR) environment, a measure of pressure responses is necessary, since in this case the correlation coefficient gives a large peak value, which

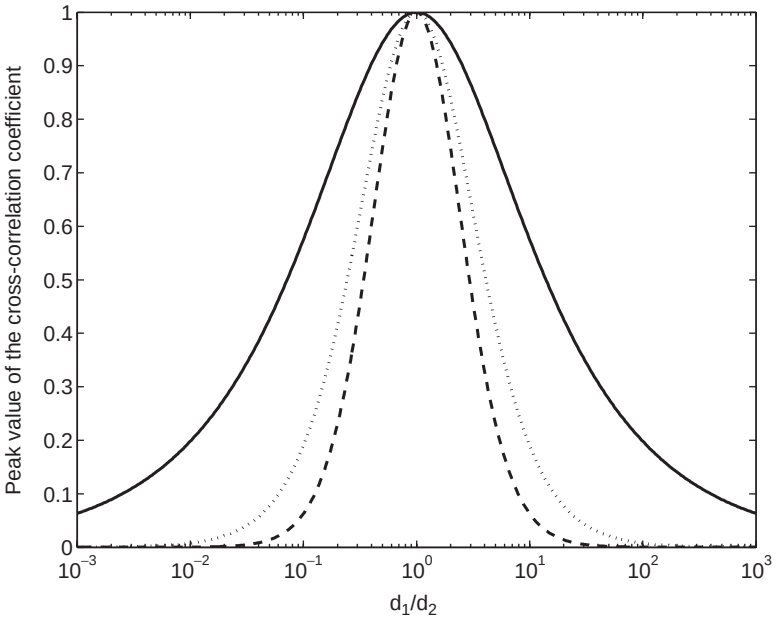

Fig. 4. Peak value of the cross-correlation coefficient as a function of the ratio of the distances d_1 and d_2. Pressure (—), velocity (……) and acceleration (----).

is less sensitive to the relative distances of the sensor locations. In practical situations, the achievement of cross-correlation coefficients with clear (or definite) peaks will be further constrained because of band-pass filtering and background noise.

The behaviour of the peak value of the cross-correlation coefficient exhibited in Fig. 3 is easily explained in physical terms. When leak sensors are equidistant from the leak source, leak signals will be identical and therefore will lead to the largest peak cross-correlation coefficient. As the ratio between leak sensors distances, d_1/d_2, becomes larger or smaller, the similarity between the sensor signals diminishes due to the frequency dependence of attenuation rates. Pressure responses give the highest peak cross-correlation coefficient because they have the least high-frequency content and hence are least affected by attenuation.

To accurately determine the position of a leak, a sharp (narrow) peak in the cross-correlation function is desirable. The way in which the cross-correlation obtained from pressure, velocity, and acceleration responses affect the peak is now investigated. We define a cross-correlation width, $\Delta\tau$, as the time between the first two zero crossings given by $\rho_{x_1x_2}(\tau_{\text{peak}} \pm \Delta\tau/2) = 0$. The behaviour of $\Delta\tau$ for the various correlation functions is as follows

1. For pressure responses, Eq. (18a) shows that the width $\Delta\tau$ is undefined as the cross-correlation has no zero crossings, and hence $\Delta\tau = \infty$. However, the 3dB width of the cross-correlation is found to be [11]

$$\Delta\tau \approx 2\beta d. \tag{20a}$$

2. For velocity responses, from Eq. (18b), the width, $\Delta\tau$ is determined to be

$$\Delta\tau = \frac{2}{\sqrt{3}}\beta d. \tag{20b}$$

3. For acceleration responses, from Eq. (18c), $\Delta\tau$ is determined to be

$$\Delta\tau = \frac{2}{\sqrt{5+2\sqrt{5}}}\beta d. \tag{20c}$$

For different sensor signals, it can be seen that the width of the peak in the cross-correlation function is proportional to the product βd. Thus, for leak detection in pipes with small attenuation (small β), as in the case of metal pipes, a sharp peak can be easily achieved using the correlation technique. In contrast, for plastic pipes with large attenuation (large β), a relatively short distance between two sensor locations is often required for the estimation of time delay from the cross-correlation function.

By comparing the cross-correlation width given by Eqs. (20a–c), it can be seen that the correlation between acceleration signals provides the sharpest peak in the correlation function, while the broadest peak occurs for pressure signals. It is found, therefore, that a sharp peak can be achieved by using the acceleration responses at the expense of a low peak value of the correlation coefficient, as shown in Fig. 3.

4. Experimental work

Tests were carried out at a leak detection facility at an experimental site located at a National Research Council site in Canada. The description of the test site and measurement procedures are detailed in Ref. [4]. Signals from a joint leak were measured using hydrophones and accelerometers. The hydrophones and accelerometers were both attached to two fully pressurised fire hydrants. Referring to Fig. 1, the distance d between the two sensor signals was 102.6 m, and the distance d_1 from the leak to sensor 1 was 73.5 m. The signals were each passed through an anti-aliasing filter with the cut-off frequency set at 200 Hz. Hydrophone-measured signals of 66-s duration were then digitised at a sampling frequency of 500 samples/s. The same sampling frequency was applied to the accelerometer-measured signals for the time duration of 60 s.

Spectral analysis was performed on the digitised data using a 1024-point FFT, and a Hanning window and power spectrum averaging were applied. The propagation wavespeed can be determined from the cross-spectral density between two sensor signals. The phase spectra obtained from the hydrophone and accelerometer-measured signals are shown in Figs. 5(a) and (b). As discussed in Ref. [11], based on the slope of the unwrapped phase angle plotted in Figs. 5(a) and (b), the wavespeed calculated is 479 and 484 m/s for hydrophone and accelerometer-measured signals respectively. The attenuation factor β is 2.26×10^{-4} s/m [7].

Noting that the measured signals were dominated by the ambient noise at low frequencies and attenuated at high frequencies [11], filtering operations were performed on the digitised sensor signals before conducting the time-domain cross-correlation. The sensor signals were then passed through high- and low-pass fourth order Butterworth filters. The cut-off frequencies of the digital filters were chosen using the phase spectrum between two sensor signals plotted in Figs. 5(a) and (b). The lower and upper cut-off frequencies were set at 10 and 50 Hz for hydrophone-measured signals, and 30 and 140 Hz for accelerometer-measured signals. The cross-correlation coefficients were computed using segment averaging via a 1024-point FFT and the circular effect of the FFT was reduced by 50% zero padding in each segment record.

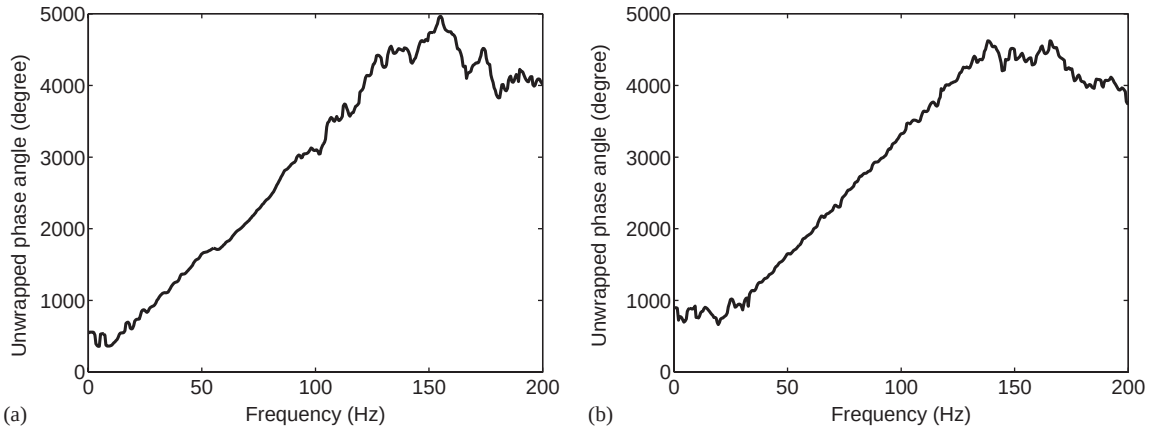

Fig. 5. Unwrapped phase angle for (a) hydrophone-measured signals; (b) accelerometer-measured signals.

If the signals are band-pass filtered using an ideal filter, $G(\omega)$, which is equal to unity if $\omega_0 \leqslant |\omega| < \omega_1$ and zero otherwise, the cross-correlation function becomes

$$R_{x_1x_2}(\tau) = (-1)^n A_n^2 R_{ll}(\tau) \otimes \frac{\mathrm{d}^{2n}\psi(\tau)}{\mathrm{d}\tau^{2n}} \otimes g(\tau) \otimes \delta(\tau + T_0), \tag{21}$$

where

$$g(\tau) = F^{-1}\{G(\omega)\} = \frac{B}{\pi} \frac{\sin(B\tau/2)\cos(\omega_c\tau)}{B\tau/2}$$

the frequency band $B = \omega_1 - \omega_0$ and the central frequency $\omega_c = (\omega_0 + \omega_1)/2$. It can be seen that the effect of band-pass filtering is to introduce a ripple with frequency ω_c into the cross-correlation modulated by the bandwidth B. Eq. (21) also shows that the Dirac delta function is further smeared by the introduction of band-pass filtering. When $S_{ll}(\omega) = S_0$, Eq. (21) becomes

$$R_{x_1x_2}(\tau) = (-1)^n A_n^2 S_0 \frac{\mathrm{d}^{2n}\psi(\tau)}{\mathrm{d}\tau^{2n}} \otimes g(\tau + T_0). \tag{22}$$

Following a similar analysis, the auto-correlation $R_{xx}(\tau)$ is found to be

$$R_{xx}(\tau) = (-1)^n A_n^2 S_0 \frac{\mathrm{d}^{2n}\varphi(\tau)}{\mathrm{d}\tau^{2n}} \otimes g(\tau). \tag{23}$$

Eqs. (22), (23) and (2) can be combined to determine the cross-correlation coefficient when the leak noise signals are band-pass filtered.

The predicted and measured cross-correlation coefficients using the hydrophone-measured signals are plotted in Figs. 6(a) and (b), respectively. To compare the experimental results with the corresponding theoretical predictions, the effect of the background noise on the theoretical predictions is taken into account by setting the peak values of the cross-correlation coefficients to

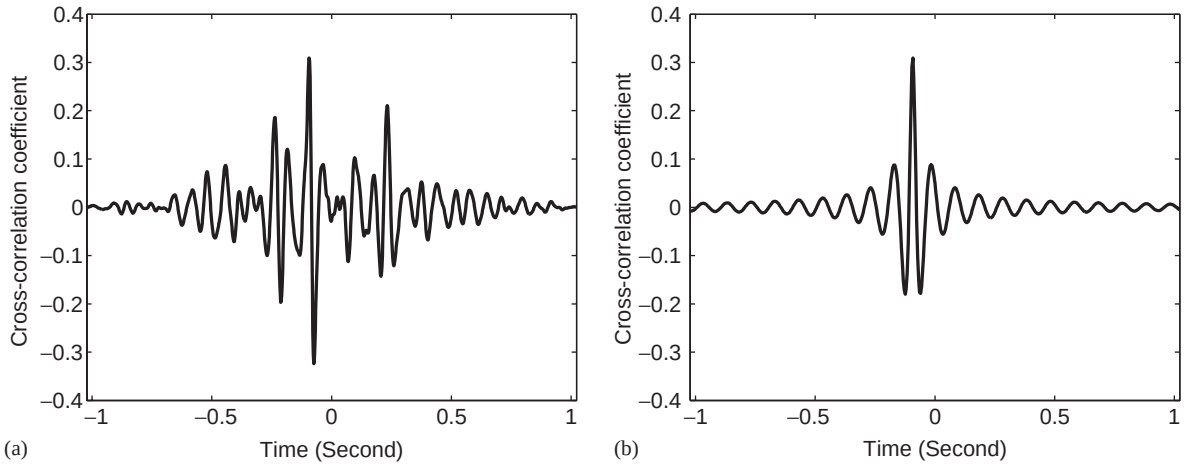

Fig. 6. Cross-correlation using hydrophone-measured signals: (a) cross-correlation coefficient; (b) theoretical prediction. The pass band of the ideal filter is 10–50 Hz.

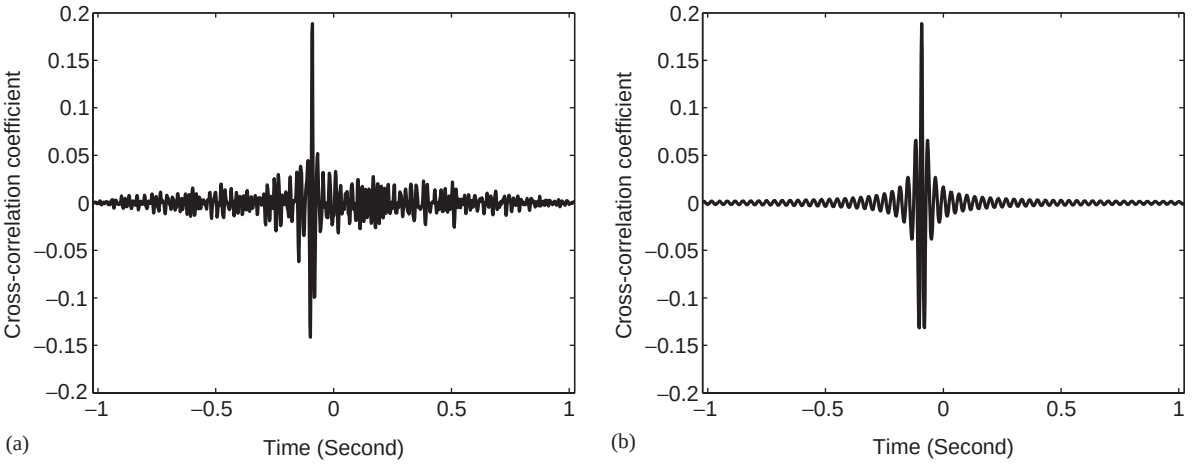

Fig. 7. Cross-correlation using accelerometer-measured signals: (a) cross-correlation coefficient; (b) theoretical prediction. The pass band of the ideal filter is 30–140 Hz.

be the same as those of the experimental results. In Appendix B, it is shown that an estimate of the SNR at a measurement position can be simply determined from the ratio of the peak values of the experimental result of the correlation coefficient and its corresponding theoretical prediction. The SNR was found to be −6.7 and 2.7 dB at positions where hydrophones 1 and 2 were attached respectively. For the measured signal, the time delay is −0.094 s and the position of the leak relative to point 1 is calculated to be 73.8 m. Comparison of Figs. 6(a) and (b) show the same oscillatory behaviour of the correlation coefficients. The differences between the predictions and the experimental results are most likely due to the effect of the background noise and reflections from discontinuities in the pipe.

The cross-correlation coefficient using accelerometer-measured signals and the corresponding theoretical prediction is plotted in Fig. 7. As before, theoretical predictions of the cross-correlation coefficients are adjusted to account for the presence of background noise. Compared with the hydrophone-measured signals plotted in Fig. 6(a), Fig. 7(a) show that the correlation coefficient obtained from accelerometer-measured signals produces a more pronounced but lower peak value. The distance d_1 is found to be 73.1 m, which is determined from the time delay of −0.090 s. The corresponding theoretical prediction plotted in Fig. 7(b) illustrates very similar high-frequency behaviour of the correlation coefficient. In this case, the SNR were found to be −10.9 and 14.6 dB at positions where accelerometers 1 and 2 were attached.

5. Conclusions

Based on an analytical model of the cross-correlation of pressure responses established in an earlier study, the effectiveness of the correlation technique using different acoustic/vibration sensors has been evaluated for leak detection in plastic water distribution pipes.

Theoretical predictions of the correlation coefficients of pressure, velocity and acceleration responses show the following:

- The use of pressure signals leads to the highest peak cross-correlation coefficient. Therefore, a measure of pressure responses using hydrophones would be the most suitable for locating leaks having small SNR. This is consistent with practical experience.
- Pressure signals are the least sensitive to the relative positions of the sensors and therefore are the most suitable for extreme positions. Good levels of peak cross-correlation coefficient (e.g., greater than about 0.5) are only possible when the ratio of distances satisfy $1/10 \leqslant d_1/d_2 \leqslant 10$, $1/4 \leqslant d_1/d_2 \leqslant 4$ and $1/3 \leqslant d_1/d_2 \leqslant 3$ for pressure, velocity and acceleration responses, respectively. In practice, these limits will be less stringent due to the limited bandwidth of the leak source and background noise.
- The use of acceleration signals results in the sharpest peak of the cross-correlation coefficient. It also exhibits the least spreading of the envelope. This suggests that accelerometers are most suitable in multi-leak and coherent noise situations.

The theoretical predictions have been validated to some extent by comparison with results obtained using real leak signals from a test site in Canada measured by hydrophones and accelerometers.

Acknowledgements

The authors gratefully acknowledge the support of the EPSRC under Grant GR/R13937/01.

Appendix A. Wave propagation and attenuation in fluid-filled plastic pipes

At low frequencies, well below the pipe ring frequency, the predominantly fluid-borne wave, which is responsible for the propagation of leak noise, has a wavenumber k given by [6,10,11]

$$k^2 = k_f^2\left(1 + \frac{2Ba}{Eh + \mathrm{i}\eta Eh}\right), \tag{A.1}$$

where k_f is the free-field fluid wavenumber, η is the loss factor of the pipe wall, and B is the fluid bulk modulus of elasticity. The real part of the wavenumber is related to the wavespeed by

$$\mathrm{Re}\{k\} = \frac{\omega}{c}, \tag{A.2}$$

where c is the wavespeed given by

$$c = c_f\left(1 + \frac{2Ba}{Eh}\right)^{-1/2}, \tag{A.3}$$

and the imaginary part is related to wave attenuation by

$$\mathrm{Im}\{k\} = -\beta\omega, \tag{A.4}$$

where β is a measure of the loss within the pipe wall, which is given by

$$\beta = \frac{1}{c_f} \frac{\eta Ba/(Eh)}{\left[1 + 2Ba/(Eh)\right]^{1/2}}, \tag{A.5}$$

where c_f is the free-field fluid wavespeed. Eq. (A.3) shows that the propagation wavespeed is independent of frequency at low frequencies. The attenuation (loss) of the amplitude of the propagating wave in dB/m is given by

$$\text{Loss} = -\frac{20\text{Im}\{k\}}{\ln(10)} = 8.67\beta\omega. \tag{A.6}$$

For a typical PVC pipe with $a/h = 10$ and $E = 5 \times 10^9\,\text{N/m}^2$, $\text{Re}\{k\} \approx 3.2k_f$. Eq. (A.3) shows that the wavespeed decreases rapidly with decreasing pipe wall stiffness and Eq. (A.6) shows that wave attenuation increases with frequency.

Appendix B. Effect of the background noise on the correlation technique

The aim of this appendix is to quantify the effect of noise on the correlation technique, in which noise can be included into the analytical model of the correlation coefficient derived in Section 3. Assume that the leak signals measured by two acoustic sensors are in the presence of the background noise. This can be modelled as

$$x_1(t) = s_1(t) + n_1(t), \tag{B.1a}$$

and

$$x_2(t) = s_2(t) + n_2(t), \tag{B.1b}$$

where random processes $s_1(t)$, $s_2(t)$, $n_1(t)$ and $n_2(t)$ are stationary. If the noise at each sensor is assumed to be uncorrelated with each other and with the signals, then the cross-correlation function of signals $x_1(t)$ and $x_2(t)$ is given by

$$R_{x_1x_2}(\tau) = R_{s_1s_2}(\tau). \tag{B.2}$$

Eq. (B.2) indicates that the effect of the uncorrelated background noise can be removed when correlating the two sensor signals. Noting that $R_{xx}(0) = \sigma_x^2$, the cross-correlation coefficient $\rho_{x_1x_2}(\tau)$ including the effect of noise is given by

$$\begin{aligned}\rho_{x_1x_2}(\tau) &= \frac{R_{x_1x_2}(\tau)}{\sqrt{R_{x_1x_1}(0)R_{x_2x_2}(0)}} \\ &= \frac{\rho_{s_1s_2}(\tau)}{\sqrt{\left[1 + (\sigma_{n_1}^2/\sigma_{s_1}^2)\right]\left[1 + (\sigma_{n_2}^2/\sigma_{s_2}^2)\right]}},\end{aligned} \tag{B.3}$$

where $\sigma_{s_1}^2$, $\sigma_{s_2}^2$, $\sigma_{n_1}^2$, and $\sigma_{n_2}^2$ are the variances of signals $s_1(t)$, $s_2(t)$ and background noise signals $n_1(t)$, $n_2(t)$ respectively, $\rho_{s_1s_2}(\tau)$ is the theoretical prediction of the cross-correlation coefficient. Eq. (B.3) shows that the correlation coefficient is strongly affected by the SNR of the two measurement positions. Based on information of the acoustical characteristics of the leak signal

and the measurement positions, estimates of the SNR for sensor signals can thus be obtained from the correlation coefficients.

In the presence of the background noise, for example at sensor 1, the SNR in terms of the ratio $\sigma_{n_1}^2/\sigma_{s_1}^2$ in Eq. (B.3) is defined as

$$\mathrm{SNR} = 10\log_{10}\left(\frac{\sigma_{s_1}^2}{\sigma_{n_1}^2}\right). \tag{B.4}$$

Assuming that the noise levels at the two measurement positions are the same, i.e., $\sigma_{n_1}^2 = \sigma_{n_2}^2$, Eq. (B.3) gives

$$\left[\frac{\rho_{s_1s_2}(\tau)}{\rho_{x_1x_2}(\tau)}\right]^2 = 1 + \left(1 + \frac{\sigma_{s_1}^2}{\sigma_{s_2}^2}\right)\frac{\sigma_{n_1}^2}{\sigma_{s_1}^2} + \frac{\sigma_{s_1}^2}{\sigma_{s_2}^2}\left(\frac{\sigma_{n_1}^2}{\sigma_{s_1}^2}\right)^2, \tag{B.5}$$

where the ratio $\sigma_{s_1}^2/\sigma_{s_2}^2$ can be obtained from Eq. (23). Using the ratio of the peak cross-correlation coefficients $\rho_{s_1s_2}(\tau_{\mathrm{peak}})/\rho_{x_1x_2}(\tau_{\mathrm{peak}})$, the ratio $\sigma_{n_1}^2/\sigma_{s_1}^2$ can be determined from the quadratic Eq. (B.5). This is then substituted into Eq. (B.4) to give an estimate of the SNR at sensor 1. A similar procedure can be adopted to obtain the SNR at sensor 2.

References

[1] M. Fantozzi, G.D. Chirico, E. Fontana, F. Tonolini, Leak inspection on water pipelines by acoustic emission with cross-correlation method, *Annual Conference Proceedings, American Water Works Association, Engineering and Operations*, San Antonio, 1993, pp. 609–721.

[2] H.V. Fuchs, R. Riehle, Ten years of experience with leak detection by acoustic signal analysis, *Applied Acoustics* 33 (1991) 1–19.

[3] D.A. Liston, J.D. Liston, Leak detection techniques, *Journal of the New England Water Works Association* 106 (1992) 103–108.

[4] O. Hunaidi, W. Chu, A. Wang, W. Guan, Detecting leaks in plastic pipes, *Journal American Water Works Association* 92 (2000) 82–94.

[5] O. Hunaidi, W.T. Chu, Acoustical characteristics of leak signals in plastic water distribution pipes, *Applied Acoustics* 58 (1999) 235–254.

[6] R.J. Pinnington, A.R. Briscoe, Externally applied sensor for axisymmetric waves in a fluid filled pipe, *Journal of Sound and Vibration* 173 (1994) 503–516.

[7] Y. Gao, M.J. Brennan, P.F. Joseph, J.M. Muggleton, O. Hunaidi, A model of the correlation function of leak noise in buried plastic pipes, *Journal of Sound and Vibration* 277 (2004) 133–148.

[8] O. Hunaidi, Detecting leaks in water-distribution pipes, Construction Technology Update No. 40, National Research Council, Canada, 2000.

[9] A.V. Oppenheim, R.W. Schafer, *Digital Signal Processing*, Prentice-Hall, Englewood Cliffs, NJ, 1975.

[10] J.M. Muggleton, M.J. Brennan, R.J. Pinnington, Wavenumber prediction of waves in buried pipes for water leak detection, *Journal of Sound and Vibration* 249 (2002) 934–954.

[11] Y. Gao, M.J. Brennan, P.F. Joseph, J.M. Muggleton, Use of cross-correlation for leak detection in plastic pipes, ISVR Technical Memorandum No. 90, UK, 2002.